Measuring blood velocity using correlative spectrally encoded flow cytometry

Tal Elhanan and Dvir Yelin*

Faculty of Biomedical Engineering, Technion—Israel Institute of Technology, Haifa 32000, Israel
**Corresponding author: yelin@bm.technion.ac.il*

Received May 6, 2014; revised June 24, 2014; accepted June 25, 2014;
posted June 25, 2014 (Doc. ID 211518); published July 23, 2014

Spectrally encoded flow cytometry (SEFC) is a promising technique for imaging blood in the microcirculation. Yet, the dependency of one of the axes of the image on time prevents effective quantification of essential clinical parameters. Here, we address this challenge by splitting the optical path in an SEFC system into two parallel imaging lines, followed by straightforward data analysis for recovering the flow speed from the multiplexed data. The method is demonstrated by measuring the flow velocity of latex beads and blood cells *in vitro*. The system allows real-time velocity measurements of up to 11.7 mm/s at high spatial resolution, and could be integrated into existing SEFC systems for effectively measuring blood parameters in small capillary vessels.

OCIS codes: (120.3890) Medical optics instrumentation; (170.1790) Confocal microscopy; (170.4580) Optical diagnostics for medicine; (280.2490) Flow diagnostics.
http://dx.doi.org/10.1364/OL.39.004424

Quantitative information on blood composition and blood cell morphology is frequently used for patient diagnosis [1] using flow cytometry [2] complemented by chemical analysis and optical microscopy [3]. In recent years, several methods for obtaining useful clinical data from small drops of extracted blood have been developed [4–6], reducing pain and anxiety to patients. Noninvasive optical techniques for measuring key clinical indices of blood have also been demonstrated and shown clinically useful, including pulse oximetry [7], photothermal imaging [8], and orthogonal polarized spectral imaging [9]. While limited by the accuracy of their data, these technologies are attractive for many applications that require real-time diagnosis, involve difficult extraction of blood, or where proper sample handling cannot be maintained.

Recently, a novel technique termed spectrally encoded flow cytometry (SEFC) has been shown effective for noninvasive, high-resolution imaging of blood flowing in the microcirculation [10]. Using a portable handheld probe, this technique uses a diffraction grating and a high numerical aperture (NA) lens to image reflectance from a spectrally encoded confocal line that is positioned at the cross section of a small blood vessel. As cells within the blood stream cross the spectrally encoded line, backscattered light is repeatedly recorded to form a two-dimensional confocal image of the cells without additional mechanical scanning. When the spectrally encoded line is positioned perpendicular to the direction of flow, the resulting two-dimensional SEFC data is spanned by the spectrally encoded line that encodes the y (Cartesian) coordinate while the x coordinate is encoded by time. Thus, in an uncorrected raw image, cells flowing at higher velocities appear shorter along the x axis compared with slower moving cells of similar morphology, resulting in an inability to estimate their true proportions. Perhaps more importantly, obtaining key clinical parameters that involve cell counts (e.g., red and white blood cell counts, platelets) requires knowledge of the exact imaged volume for effectively extrapolating the measured parameters to the entire body. Thus, transforming the time axis into a physical x axis requires precise, real-time measurement of the blood flow velocity across the field of view. Although non invasive flow velocity measurements in the microcirculation had been previously demonstrated using laser speckle contrast analysis [11], laser Doppler [12], and orthogonal polarized spectral imaging [9], these techniques provide only averaged measurements and would be difficult to integrate into an SEFC system.

In this Letter, we present a technique for measuring flow velocities in the microcirculation in real-time and at high spatial accuracy. Our correlative SEFC technique was inspired by the early work of Wayland and Johnson [13], in which blood flow velocities in small mesentery vessels in cats were estimated by measuring temporal correlations of the flow patterns between two nearby locations along the vessel; similarly, by splitting the imaging beam in the SEFC probe into separate paths, we demonstrate accurate velocity measurements of the imaged cells. The experimental setup of correlative SEFC, schematically illustrated in Fig. 1, is based on our current SEFC system [14] used for imaging capillary blood flow in patients. Broadband light from a fiber-coupled superluminescent diode array (Superlum S840-B-I-20, 840 nm central wavelength, 50 nm bandwidth) was collimated, magnified to 9 mm beam diameter using a 3.75× beam expander, diffracted in the y axis using a transmission

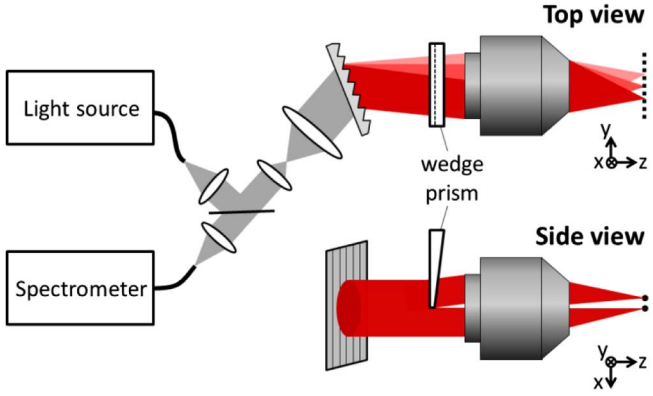

Fig. 1. Schematic illustration of the correlative SEFC optical setup.

diffraction grating (Wasatch Photonics, 1200 lines/mm), and split in the x axis using a 0.5° wedge prism (Edmund Optics, Inc.) that was inserted halfway into the beam cross section (see side view in Fig. 1). The two split halves of the beam were then focused into two equal intensity transverse lines using a water-immersion objective lens (Olympus, NA = 1.2, 60×). At the focal plane, the x axis separation between the on-axis and the off-axis spectrally encoded lines was approximately 24 μm, measured by translating a sharp edge along the x axis in the focal plane. Backscattered light from the tissue was collected by the objective lens and directed by a beam splitter to a single-mode fiber. The collected light was then analyzed by a high-speed spectrometer comprising a collimating lens (50 mm focal length), a transmission diffraction grating (1800 lines/mm), and a line-CCD camera (e2v, Aviiva EM4). Note that the setup in Fig. 1 has many similarities to a previously published SEFC system [14], with the important exception of the 0.5°-angle wedge prism; without the prism, the spectrometer records the reflections along a single spectrally encoded line, forming an image of the cells flowing across it. With the wedge prism inserted into the beam, reflections from both lines are combined on the spectrometer camera, forming a line-image that is the coherent summation of the reflections from both spectrally encoded lines.

The insertion of the round, 25-mm-diameter wedge prism into the optical path changes the original circular beam aperture into two smaller, slightly distorted D-shaped apertures. The effect of the prism on the two point-spread functions (PSFs) was simulated by solving the Fresnel integral for the split beams (Fig. 2). Compared with the PSF resulted from the uncropped aperture (leftmost panel), the resulting light distributions at the focal plane showed approximately 2-fold loss of resolution in the horizontal (x) axis while the y (wavelength) axis had remained nearly unaffected [15]. Close inspection of the speckle patterns resulted from imaging (NA = 0.65) a scattering resolution target (Fig. 2, insets) has confirmed the asymmetric 2-fold resolution drop. We note here that common resolution measurements using reflective targets are not feasible with this configuration due to inherent coupling between the two beams, which prevents specular reflections from being collected by the fiber aperture.

Measuring the flow velocity of 6.4-μm-diameter latex beads was obtained by placing the two spectrally encoded lines approximately 300 μm below the front surface of a flow chamber (0.8 mm × 5 mm × 50 mm, ibidi GmbH, μ-Slide I 0.4 Luer). The resulting correlative SEFC images [Fig. 3(a)] clearly showed the flowing beads, where each bead in the image essentially appears twice: first while reflecting light from the first spectrally encoded line, and later when reflecting light from the second off-axis line. The two images of each particle were also shifted in the y axis, most likely due to a small shift between the wavelength-encoded lines [Fig. 3(b), top panel] caused by a slight misalignment of the wedge prism. Another possibility for a y axis shift, which could occur mainly during *in vivo* measurements, is that the lines are not perfectly perpendicular to the direction of flow [Fig. 3(b), bottom panel].

The flow velocity v was calculated from a two-dimensional autocorrelation of a 1024-line crop of the raw data, using $v = L/\tau$, where L denotes the separation between the spectrally encoded lines and τ denotes the measured time-delay coordinate of the first autocorrelation peak [Fig. 3(c)]. The results of five measurements of different flow velocities are plotted in Fig. 3(d) against the expected velocities calculated using the parameters of the syringe pump (Harvard Apparatus), and by considering a laminar parabolic flow approximately 300 μm below the front chamber wall. The plot shows a small systematic error of approximately 15% between the measured and expected velocities [Fig. 3(d)], most likely due to overestimation of the exact imaging depth; such error could be corrected using straightforward system calibration. Vertical error bars in Fig. 3(d) include the width of the autocorrelation peaks and the estimated error in measuring the distance between the spectrally encoded lines. Horizontal error bars include the estimated errors of the pump velocity and imaging depth.

To demonstrate velocity measurement of blood flow, blood from a venipuncture of a healthy donor was diluted (1:5) with phosphate buffered saline (PBS) and was pumped through the flow chamber. Due to the high forward scattering of the red blood cells, which rapidly reduced image quality with depth, imaging was performed just below (approximately 10 μm) the front chamber wall. Numerous red blood cells were clearly visible in the raw image [Fig. 4(a)], most appeared twice with consistent shifts in the time (x axis) and small constant shifts

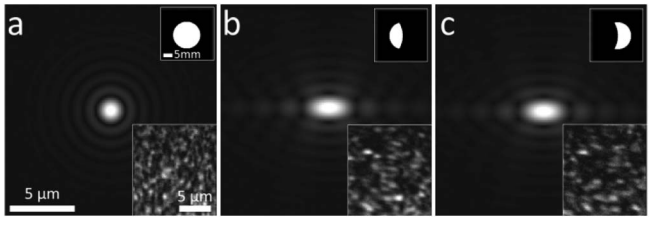

Fig. 2. Point-spread functions resulting from (a) a full aperture of an uncropped SEFC beam, (b) the cropped aperture of the beam passing through the wedge prism, and (c) the cropped aperture of the remaining on-axis beam. Upper-right insets, simulated apertures. Lower-right insets, corresponding speckle images of a scattering target.

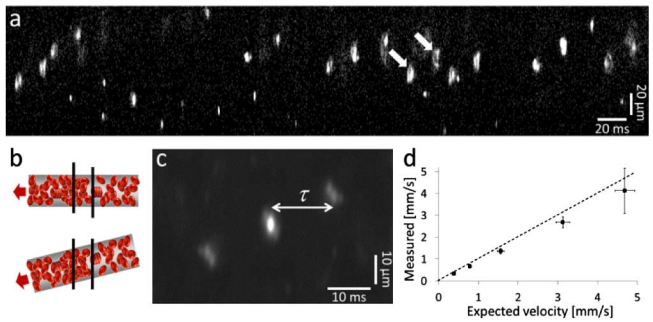

Fig. 3. Velocity measurement of flowing latex beads. (a) Correlative SEFC raw image. Arrows mark two images of the same bead. (b) Schematic illustration of the potential imaging configurations that result in the observed y axis shift. (c) Two-dimensional autocorrelation of the raw data. τ denotes the separation between the two peaks. (d) Measured versus expected velocities show small and consistent deviation from the identity (dashed) line.

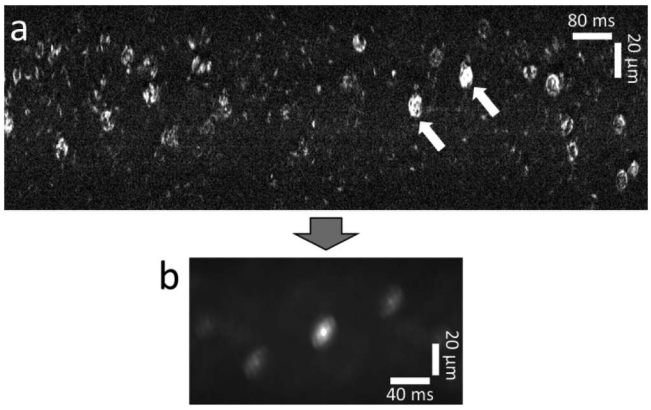

Fig. 4. Correlative SEFC imaging of diluted blood flow *in vitro*. (a) Raw data, arrows mark double images of a red blood cell. (b) Two-dimensional autocorrelation image of the raw data, corresponding to a velocity of 0.45 ± 0.13 mm/s.

in the wavelength-encoded y axis. Some cells appear only once, most likely due to a small component of the flow vector in the depth dimension (z axis). As evident from the first autocorrelation peak [Fig. 4(b)], averaged blood velocity was approximately 0.45 mm/s with an estimated error (peak width) of ± 0.13 mm/s. Due to the strong influence of the nearby chamber wall, this velocity was difficult to compare with theoretical predictions [16].

The main advantage of correlative SEFC in measuring blood velocity is that it relies on high-resolution confocal images that allow effective extraction of microscopic flow. When desired, during an SEFC imaging session, the operator may insert the wedge prism for measuring the flow velocity during a few seconds, and then remove it for continuing high-resolution imaging using conventional SEFC. Note that, in small-diameter capillary vessels, the velocity would not be uniform across the image: in the wavelength-encoded y axis, the flow is expected to have varying characteristics (plug and parabolic flow [17]) while, in the time (x) axis, it may vary due to residual pulsation in arterioles [17]. A windowed autocorrelation [18,19] of the raw images would thus be more appropriate for future *in vivo* applications for assessing velocities at higher spatial and temporal accuracies. Due to the relatively large number of pixels per cell (8–12 in the x axis), autocorrelation errors are expected to have no bias [20].

The maximal flow velocity that could be measured using correlative SEFC is given by:

$$v_{\max} = \frac{fd}{N_{\text{cell}}}, \tag{1}$$

where f denotes the camera line rate, d the average cell diameter, and N_{cell} denotes the number of pixels sampling each blood cell ($N_{\text{cell}} > 2$) [20]. Using $f = 5$ kHz, $d = 7$ μm, and $N_{\text{cell}} = 3$, we obtain a maximum velocity of 11.7 mm/s, considerably higher than the typical velocities in venules and in small arterioles [17]. The efficiency of correlative SEFC in measuring velocities also depends on the exact distance between the spectrally encoded lines; short separations are preferable for reducing the effect of the axial component of the flow while line separation must exceed cell size for separating between the autocorrelation peaks. Other means for improving the accuracy of the flow measurement include using conventional beam splitters and mirrors, which, despite some signal loss and added complexity, would maintain the full apertures of both beams and, by allowing sufficient optical path difference between the beams, prevent undesired interference effects. Finally, correlative SEFC could be used as a standalone technique for measuring blood flow velocities in the microcirculation with extremely high accuracy; however, additional experiments are required to determine the true potential of this approach and to understand its limitations, primarily due to the small field of view and the high sensitivity of the results to the actual depth of imaging into the vessel.

In summary, a technique for measuring the velocity of blood cells using SEFC system was presented and experimentally demonstrated *in vitro*. Using two parallel spectrally encoded lines positioned across a flow chamber, we demonstrated velocity measurements of latex bead and blood cells. The technique could be easily integrated into existing SEFC systems, enabling the measurement of useful clinical parameters for effective, pain-free patient diagnosis.

The authors thank Lior Golan for valuable discussions and technical assistance. The study was funded in part by the European Research Council Starting Grant (239986) and supported in part by the Lorry I. Lokey Interdisciplinary Center for Life Sciences and Engineering.

References

1. V. Hoffbrand and P. Moss, *Essential Haematology* (Wiley, 2011), Vol. **39**.
2. C. D. Jennings and K. A. Foon, Blood **90**, 2863 (1997).
3. B. J. Bain, N. Engl. J. Med. **353**, 498 (2005).
4. C. Briggs, S. Kimber, and L. Green, Br. J. Haematol. **158**, 679 (2012).
5. B. A. Ekberg, U. D. Larsen, and N. Fogh-Andersen, Point Care **4**, 64 (2005).
6. C. van Berkel, J. D. Gwyer, S. Deane, N. Green, J. Holloway, V. Hollis, and H. Morgan, Lab Chip **11**, 1249 (2011).
7. I. Yoshiya, Y. Shimada, and K. Tanaka, Med. Biol. Eng. Comput. **18**, 27 (1980).
8. V. P. Zharov, E. I. Galanzha, and V. V. Tuchin, Opt. Lett. **30**, 628 (2005).
9. W. Groner, J. W. Winkelman, A. G. Harris, C. Ince, G. J. Bouma, K. Messmer, and R. G. Nadeau, Nat. Med. **5**, 1209 (1999).
10. L. Golan and D. Yelin, Opt. Lett. **35**, 2218 (2010).
11. J. D. Briers and S. Webster, J. Biomed. Opt. **1**, 174 (1996).
12. A. K. Murray, A. L. Herrick, and T. A. King, Rheumatology **43**, 1210 (2004).
13. H. Wayland and P. C. Johnson, J. Appl. Physiol. **22**, 333 (1967).
14. L. Golan, D. Yeheskely-Hayon, L. Minai, E. J. Dann, and D. Yelin, Biomed. Opt. Express **3**, 1455 (2012).
15. C. J. Sheppard, W. Gong, and K. Si, Opt. Express **16**, 17031 (2008).
16. R. Fox, A. McDonald, and P. J. Pritchard, *Introduction to Fluid Mechanics*, 6th ed. (Wiley, 2006).
17. A. S. Popel and P. C. Johnson, Annu. Rev. Fluid Mech. **37**, 43 (2005).
18. C. E. Willert and M. Gharib, Exp. Fluids **10**, 181 (1991).
19. D. P. Hart, J. Vis. **3**, 187 (2000).
20. J. Westerweel, in *Laser Techniques Applied to Fluid Mechanics*, R. J. Adrian, D. F. G. Durao, F. Durst, M. V. Heitor, M. Maeda, and J. H. Whitelaw, eds. (Springer, 2000), pp. 37–55.